Research Article Vol. 28, No. 3 / 3 February 2020 / Optics Express 3073
Optics EXPRESS

# On the constraints of electromagnetic multipoles for symmetric scatterers: eigenmode analysis

ZHONGFEI XIONG,[1,4] QINGDONG YANG,[1,4] WEIJIN CHEN,[1] ZHUORAN WANG,[1] JING XU,[1,2,5] WEI LIU,[3] AND YUNTIAN CHEN[1,2,6]

[1]School of Optical and Electronic Information, Huazhong University of Science and Technology, Wuhan 430074, China
[2]Wuhan National Laboratory of Optoelectronics, Huazhong University of Science and Technology, Wuhan, China
[3]College for Advanced Interdisciplinary Studies, National University of Defense Technology, Changsha, Hunan 410073, China
[4]These two authors contributed equally to this work
[5]jing_xu@hust.edu.cn
[6]yuntian@hust.edu.cn

**Abstract:** The scattering and resonant properties of optical scatterers/resonators are determined by the relative ratios among the associated multipole components, the calculation of which usually is analytically tedious and numerically complicated for complex structures. Here we identify the constraints as well as the relative relations among electromagnetic multipoles for the eigenmodes of symmetric scatterers/resonators. By reducing the symmetry properties of the vector spherical harmonic waves to those of the modified generating functions, we systematically study the required conditions for electromagnetic multipoles under several fundamental symmetry operations, i.e., 2D rotation and reflection operations and 3D proper and improper rotations. Taking a 2D scatterer with $C_{4v}$ as an example, we show that each irreducible representation of $C_{4v}$ can be assigned to corresponding electromagnetic multipoles, and consequently the constraints of the electromagnetic multipoles can be easily extracted. Such group approach can easily be extended to more complex 3D scatterers with higher symmetry group. Subsequently, we use the same procedure to map out the complete relation and constraint on the electromagnetic multipoles of a 3D scatterer imposed by $D_{3h}$ symmetry. Our theoretical analyses are in perfect agreements with the fullwave finite element calculations of the eigenmodes of the symmetric scatters.



## 1. Introduction

Symmetry principles have played indispensable roles in simplifying complex problems in all different branches of physics [1–3]. The systematic symmetry arguments applied in physics were first developed by Winger to examine the electronic wave function of Hydrogen atoms [4]. Later on, various symmetry arguments have been developed to simplify our understanding of different phenomena and have also been widely used as general guidelines to conceive practical devices in electronics, acoustics, optics and many others [5–9]. In optics, symmetry arguments mostly are used to understand band degeneracy [10,11] and to classify the eigenmodes in periodic optical structures [12,13]. Practically, group approaches were also used to simplify the calculations of optical properties [14], i.e., the optical local density of states in complex structures [15]. Recently, the symmetry arguments are also used to analyze the Bloch mode vortices [16] and examine the polarization properties of the far-field pattern of photonic crystal slab structures [17–19].

Despite the larger amount of work devoted to periodic optical structures, the classification of modal properties from symmetry perspective for finite-size scattering objects, i.e., the single individual optical scatterer or a cluster of optical scatterers, are just a few, in which the

#382239 https://doi.org/10.1364/OE.382239
Journal © 2020 Received 5 Nov 2019; revised 20 Dec 2019; accepted 3 Jan 2020; published 22 Jan 2020

Optics EXPRESS

symmetry arguments are implicitly used, such as the calculation of scattering coefficients of the electromagnetic multipoles. It is also shown by earlier work that each electromagnetic multipole in different directions has different phases, depending on the parity of the multipole [20]. Interestingly, recent work also shows that electromagnetic multipoles, as well as the symmetric relations among electromagnetic multipoles can be crucial to reveal the type and global features of the far-field singularities, i.e., the distribution and the total indices of V-points and C-points on the momentum sphere [21]. In addition, the symmetric relations among electromagnetic multipoles lead to novel phenomena and useful applications [22], i.e., directional emission and wavefront engineering [23–29]. Considering the relevance of the optical properties of finite system, thereby it is natural and useful to use the symmetry principle to finite scattering objects [30].

In the paper, we aim to calculate the relation among the coefficients of multipoles from symmetry arguments for finite-size optical systems using eigenmode analysis. Though the symmetry of multipoles is shown in many earlier works [31], with the assistance of group theory, we build the subtle connections among different electromagnetic multipoles imposed by the spatial symmetry of the geometrically regular optical systems that have a finite size. Specifically, we use the point group associated with finite-size optical structures as a powerful tool (1) to identify the existences of certain electromagnetic multipoles, (2) to reveal the hidden connections among different electromagnetic multipole components, and (3) to give explicit constraints on the multipolar coefficients dictated by symmetry.

The paper is organized as follows. In Section 2, we outline the fundamentals of electromagnetic multipoles, symmetry operations, and the procedures of using group theory to obtain the constraints among different electromagnetic multipoles of symmetric scatters. In Section 3, we illustrate how the group approach is applied to extract the relative relations among electromagnetic multipoles for a 2D $C_{4v}$ scatterer and a 3D $D_{3h}$ scatterer, as benchmarked against fullwave numerical simulations. Finally, the paper is concluded in Section 4.

## 2. Theory

### 2.1. Applications of symmetry principle and group theory in optics

In the calculation of the eigenmodes of the symmetric scatterers, the Maxwell's equations can be reformulated into a Hamiltonian problem defined by $H(\boldsymbol{r})$, i.e., $H(\boldsymbol{r})\phi(\boldsymbol{r}) = \lambda\phi(\boldsymbol{r})$, where $\phi(\boldsymbol{r})$ is the eigenmode of the symmetric scatter with eigen-frequency given by $\lambda$. We know that $H(\boldsymbol{r})$ depends on the material properties and the scatterer geometry. In our problem, if a given symmetry operation transforms the overall system to itself, $H(\boldsymbol{r})$ is invariant under such symmetry operation $\boldsymbol{P}$, i.e., the Hamiltonian $H(\boldsymbol{r})$ and $\boldsymbol{P}$ fulfills the relation given by $\boldsymbol{P}H(\boldsymbol{r})\boldsymbol{P}^{-1} = H(\boldsymbol{r})$. All the symmetry operations which let $H(\boldsymbol{r})$ be invariant form a group. Importantly, the irreducible representations of this group have one-to-one correspondence to the eigenmodes determined by $H(\boldsymbol{r})$ due to the commutativity between $H(\boldsymbol{r})$ and $\boldsymbol{P}$. Moreover, the eigenmode of $H(\boldsymbol{r})$ transforms identically to that of the corresponding irreducible representation of the symmetry operation $\boldsymbol{P}$[32]. Namely, the symmetric properties of the eigenmode of $H(\boldsymbol{r})$ can be classified in the same fashion as the irreducible representations, as summarized in the character tables. Consequently, with the assistance of multipolar decomposition, i.e., $\phi = aM_{lm} + bN_{lm}$, one is ready to identify constraints of the multipolar components imposed by the symmetry operation. In our work, we map out all the possible fundamental symmetry operations in both 2D and 3D as well as the constraints on the multipolar components. Those fundamental symmetry operations can be used as building blocks to more complex symmetric scatterers.

For self-consistency, we next introduce the basic concept of the group theory [33], as well as the basic idea of applying group theory to the problems in optics and photonics. All the symmetry operations $\boldsymbol{P}$ associated with $H(\boldsymbol{r})$ form a group, such as rotation and mirror operations in a point group. Under certain properly selected basis functions, each operation can be represented

Optics EXPRESS

by a matrix, which can be further used to investigate symmetry properties of the eigenmodes associated with $H(\boldsymbol{r})$. As the basis functions vary, the matrix representation may also vary. However, an important quantity of the matrix representation of a certain symmetry operation is conserved despite the variation of the basis functions. The conserved quantity is the trace of the matrix representation, which is also coined as the character of the matrix representation. By similarity transformation, the matrix representation can be transformed into direct sum of the block matrices, which are called irreducible representations if the matrix representation cannot be decomposed further. Mathematically, those symmetry operations form a class, if the corresponding matrix representations can be transformed into each other by similarity transformation, the transformation matrix of which is the matrix representation of one of the group elements. Interestingly, all the important properties associated with the symmetry group can be extracted from the character tables [2]: (1) the character table lists all the irreducible representations and the characters row-by-row, i.e., which essentially corresponds to different symmetric type of the eigenmode of the scatterer in our paper; (2) each column represents a class of the group; (3) as for a specific irreducible representation (row number fixed), the character in different column is to describe the conserved quantity of matrix representation for different class, and thus reflects the symmetric properties of that irreducible representation under the symmetric operation belonging to different class.

We shall directly use character tables to classify the eigenmodes of the scatterer, the symmetric features of which can be obtained from the character of the corresponding symmetry operation (class). In the following, we will apply the character table to study the modal symmetry for the eigenmodes of the symmetric scatterers. Notably, for any given large symmetry group, it can be divided into a number of subgroups, which correspond to a few fundamental symmetry operations that can be used as building blocks for large symmetry group. In the following, we examine the constraints on the electromagnetic multipoles of the eigenmodes imposed by those fundamental symmetric operations. To this end, we first recall the symmetric properties as well as the properties under a certain symmetric operation of the electromagnetic multipoles.

### 2.2. Electromagnetic multipoles and generating functions

The electromagnetic multipoles, as a fundamental tool in optics, usually refer to the $2D$ vector cylindrical harmonic waves in the cylindrical coordinate $(r, \phi, z)$ with $z$-translation symmetry, or the 3D vector sphere harmonic waves in the spherical coordinate $(r, \phi, \theta)$. Electromagnetic multipoles can be grouped into magnetic and electric types, the electric and magnetic multipoles are given by vector spherical (cylindrical) harmonics $N_{(l,m)}$ ($N_m$) and $M_{(l,m)}$ ($M_m$), respectively. Explicitly, $M_{(l,m)}$ and $N_{(l,m)}$ are given via the generating functions $\psi_{(l,m)}$($l$ is absent in 2D) [20],

$$\boldsymbol{M}_{(l,m)} = \nabla \times \left(\boldsymbol{c}\psi_{(l,m)}\right), \quad \boldsymbol{N}_{(l,m)} = \frac{\nabla \times \boldsymbol{M}_{(l,m)}}{k}, \tag{1}$$

where $\boldsymbol{c}$ is the pilot vector ($\boldsymbol{c} = \boldsymbol{z}$ in 2D and $\boldsymbol{c} = \boldsymbol{r}$ in 3D), $k$ is vacuum wavenumber. The generating functions in 2D case are $\psi_m = Z_m(kr)\, e^{im\phi}$, where $Z_m(kr)$ is Bessel or Hankel function. As such, the 2D scattering electric field $\boldsymbol{E}_s$ and magnetic field $\boldsymbol{H}_s$ can be expanded into electromagnetic multipoles as [34]

$$\boldsymbol{E}_s = -\sum_m E_m \left[a_m \boldsymbol{N}_m^{(3)} + b_m \boldsymbol{M}_m^{(3)}\right], \tag{2}$$

$$\boldsymbol{H}_s = \frac{ik}{\omega\mu_0} \sum_m E_m \left[b_m \boldsymbol{N}_m^{(3)} + a_m \boldsymbol{M}_m^{(3)}\right], \tag{3}$$

where the superscripts of $\boldsymbol{N}_m^{(3)}$ and $\boldsymbol{M}_m^{(3)}$ indicate the first kind Hankel function $H_m^{(1)}$ used in the generating functions $\psi_m$, and $E_m = E_0\,(-i)^m\,/k$ with $E_0$ a constant.

Optics EXPRESS

The 3D generating functions are scalar spherical harmonics $\psi_{(m,l)} = e^{im\phi} P_l^m(\cos\theta)\, z_l(kr)$, where $P_l^m(\cos\theta)$ is associated Legendre function, $z_l(kr)$ is spherical Bessel or Hankel function. According to Mie theory, the scattering electric and magnetic fields of 3D scatterer are given by

$$\boldsymbol{E}_s = \sum_{l,m} iE_{(l,m)} \left[ a_{(l,m)} \boldsymbol{N}^{(3)}_{(l,m)} + b_{(l,m)} \boldsymbol{M}^{(3)}_{(l,m)} \right], \tag{4}$$

$$\boldsymbol{H}_s = \frac{k}{\omega\mu_0} \sum_{l,m} E_{(l,m)} \left[ b_{(l,m)} \boldsymbol{N}^{(3)}_{(l,m)} + a_{(l,m)} \boldsymbol{M}^{(3)}_{(l,m)} \right], \tag{5}$$

where the superscript $\boldsymbol{N}^{(3)}_{(l,m)}$ and $\boldsymbol{M}^{(3)}_{(l,m)}$ indicate the first kind spherical Hankel function $h_m^{(1)}$ is chosen in $z_l$ for the generating functions $\psi_{(l,m)}$, and $E_{(l,m)} = i^l \frac{\sqrt{(2l+1)(l-m)!}}{\sqrt{l(l+1)(l+m)!}} E_0$. By convention, $a_{(l,m)}$ is the expansion coefficient of electric multipoles of $\boldsymbol{E}$ field, and $b_{(l,m)}$ is the expansion coefficient of magnetic multipoles of $\boldsymbol{E}$ field.

For convenience, we combine the 2D and 3D generating functions, i.e., $\psi_m$ and $\psi_{(l,m)}$, with the corresponding $m$-dependent coefficients $E_m$ and $E_{(l,m)}$ as follows,

$$\tilde{\psi}_m = (-i)^m \psi_m, \tag{6}$$

$$\tilde{\psi}_{(l,m)} = i^l \frac{\sqrt{(2l+1)(l-m)!}}{\sqrt{l(l+1)(l+m)!}} \psi_{(l,m)}, \tag{7}$$

which are coined as the modified generating functions in this paper. The purpose of introducing the modified generating functions will become clear shortly.

We proceed to discuss how the symmetric properties of electromagnetic multipoles under proper rotations $\hat{O}_R$ ($\hat{O}_R \in SO(3)$ with $SO(3)$ being the 3D rotation group) and improper rotations operations $\hat{I}\hat{O}_R$ ($\hat{I}$ being the inversion operator) can be reduced to that of the corresponding generating functions. To that end, we reformulate $\boldsymbol{M}_{(l,m)} = \nabla \times \left(\boldsymbol{c}\tilde{\psi}_{(l,m)}\right)$ in Eq. (1) using the angular momentum operator $\hat{L}$, i.e., $\boldsymbol{M}_{(l,m)} = \hat{O}_M \tilde{\psi}_{(l,m)} = -\frac{i}{\hbar}\hat{L}\tilde{\psi}_{(l,m)}$, where $\hat{O}_M = -\frac{i}{\hbar}\hat{L}$ and $\hat{L} = -i\hbar \boldsymbol{r} \times \nabla$ (replacing $\boldsymbol{r}$ with $\boldsymbol{z}$ for 2D case). Taking $\hat{O}_R$ as the proper rotation operator, one can prove that $\hat{O}_R \boldsymbol{M}_{(l,m)} = \hat{O}_M \hat{O}_R \tilde{\psi}_{(l,m)}$, which is equivalent to the fact that the two operators $\hat{O}_R$ and $\hat{O}_M$ commute with each other, i.e., $\left[\hat{O}_R, \hat{O}_M\right] = \hat{O}_R\hat{O}_M - \hat{O}_M\hat{O}_R = 0$. As for the improper rotations operators $\hat{I}\hat{O}_R$, one instead can prove $\hat{I}\hat{O}_R \boldsymbol{M}_{(l,m)} = -\hat{O}_M \hat{I}\hat{O}_R \tilde{\psi}_{(l,m)}$, which amounts to the anti-commutation relation between $\hat{I}\hat{O}_R$ and $\hat{O}_M$, i.e., $\{\hat{I}\hat{O}_R, \hat{O}_M\} = \hat{I}\hat{O}_R\hat{O}_M + \hat{O}_M\hat{I}\hat{O}_R = 0$. As for the electric multipoles given by $\boldsymbol{N}_{(l,m)} = \hat{O}_N \tilde{\psi}_{(l,m)}$ with $\hat{O}_N = \frac{1}{k}\nabla \times \hat{O}_M$, one can prove that the operator $\hat{O}_N$ commutes with both $\hat{O}_R$ and $\hat{I}\hat{O}_R$, i.e., $\hat{O}_R \boldsymbol{N}_{(l,m)} = \hat{O}_N \hat{O}_R \tilde{\psi}_{(l,m)}$ and $\hat{I}\hat{O}_R \boldsymbol{N}_{(l,m)} = \hat{O}_N \hat{I}\hat{O}_R \tilde{\psi}_{(l,m)}$, see details in Appendix A. Evidently, the symmetry properties between electric multipole $\boldsymbol{N}_{(l,m)}$ and modified generating functions $\tilde{\psi}_{(l,m)}$ with respect to proper and improper rotations are completely same, while the symmetry properties of the the magnetic multipole $\boldsymbol{M}_{(l,m)}$ are the same as that of $\tilde{\psi}_{(l,m)}$ under the proper rotation, but opposite to $\tilde{\psi}_{(l,m)}$ under improper rotations. As a result, the classification of symmetry properties of electromagnetic multipoles can simply be reduced to investigate the symmetry properties of the modified generating functions [33]. For any given large symmetry group, it can be divided into a number of subgroups, which correspond to a few fundamental symmetry groups that can be used as building blocks for complex symmetry operations. In the following, we examine the constraints on the electromagnetic multipoles of the eigenmodes imposed by those fundamental symmetric operations. To this end, we first recall the symmetric properties as well as its properties under a certain symmetric operation of the electromagnetic multipoles. In the following, we inspect how the modified generating functions in Eq. (6) transform with respect to proper and improper rotations, as such the corresponding symmetry properties of electromagnetic multipoles are extracted.

Optics EXPRESS

### 2.3. The constraints of electromagnetic multipoles by fundamental symmetry operations

#### 2.3.1. Rotation and reflection in 2D

The 2D proper rotation $\hat{O}_R$ in cylindrical coordinates (z-axis as the rotation axis) is represented as $C_{nz} : \phi \rightarrow \phi + 2\pi/n$. Acting the operation $P_{C_{nz}}$ on the modified generating functions $\tilde{\psi}_m$ leads to the following relation,

$$P_{C_{nz}}\tilde{\psi}_m = \tilde{\psi}_m\left(C_{nz}^{-1}\boldsymbol{r}\right) = e^{-im\frac{2\pi}{n}}\tilde{\psi}_m, \tag{8}$$

where $m$ is the angular quantum number of $\tilde{\psi}_m$. From Eq. (8), one concludes that $\tilde{\psi}_m$ is symmetric (antisymmetric) under rotation $C_{nz}$ depending on $m = Nn$ ( $m = \left(N + \frac{1}{2}\right)n$), where $N$ is an integer. As a result, the associated eigenmodes of scatterers with $C_{nz}$ symmetry only have electric and magnetic multipoles with $m = Nn$. The only relevant 2D improper rotation is the reflection operation, as defined by $\sigma_v : \phi \rightarrow 2\phi_0 - \phi$, where $\phi_0$ is the angle between mirror plane and $xz$ plane. As the operator $\sigma_v$ acts on $\tilde{\psi}_m$ ($m \neq 0$), one shall have

$$P_{\sigma_v}\tilde{\psi}_m = e^{2im(\phi_0-\phi)}\tilde{\psi}_m = e^{2im\phi_0}\tilde{\psi}_{-m}, \tag{9}$$

where the relationship of $\pm m$ order $\tilde{\psi}_m$ can be seen in Appendix B. All the other 2D rotations can be obtained by combining $P_{C_{nz}}$ and $\sigma_v$ together.

#### 2.3.2. Proper and improper rotations in 3D

Choosing $z$-axis as the principal axis, one notes that there are 4 fundamental 3D rotation operations in total, i.e., one proper rotation operation $C_{nz}$ and 3 improper rotation operations, i.e., $\sigma_v$, $\sigma_h$ and $I$, which are the reflection in the vertical plane, reflection in the horizontal plane, and inversion operation respectively. The 3D rotation operation $C_{nz}$ as well as its operation on $\tilde{\psi}_{(l,m)}$ are identical to its 2D counterpart, i.e., $P_{C_{nz}}\tilde{\psi}_{(l,m)} = e^{-im\frac{2\pi}{n}}\tilde{\psi}_{(l,m)}$. The definition of 3D reflection $\sigma_v$ in the vertical plane is identical to its 2D counterpart, while its operation on $\tilde{\psi}_{(l,m)}$ ($m \neq 0$) is different to its 2D counterpart, as given by

$$P_{\sigma_v}\tilde{\psi}_{(l,m)} = (-1)^m e^{2im\phi_0}\tilde{\psi}_{(l,-m)}, \tag{10}$$

due to the fact that different modified generating functions are used. In contrast to $\sigma_v$ , the reflection operation in horizontal plane, defined as $\sigma_h : \theta \rightarrow \pi - \theta$, involves the parity associated Legendre function $P_l^m(-x) = (-1)^{l+m}P_l^m(x)$. Therefore, the operation of $\sigma_h$ on $\tilde{\psi}_{(m,l)}$ is distinct to Eq. (10) and is given by

$$P_{\sigma_h}\tilde{\psi}_{(l,m)} = (-1)^{(l+m)}\tilde{\psi}_{(l,m)}. \tag{11}$$

The inversion $I$, defined as $I : \phi \rightarrow \phi + \pi$, $\theta \rightarrow \pi - \theta$ in spherical coordinate, can be seen as the combination of $\sigma_v$ and $C_{2z}$. Thus, the operation of $I$ on $\tilde{\psi}_{(m,l)}$ yields,

$$P_I\tilde{\psi}_{(l,m)} = (-1)^l\tilde{\psi}_{(l,m)}. \tag{12}$$

As a trivial application of $\sigma_h$ (inversion $I$), one immediately finds out that $\tilde{\psi}_{(l,m)}$ is symmetry/antisymmetry under the reflection operation $\sigma_h$ (the inversion operation $I$) with $l + m$ ($l$) is even/odd. It is relevant to point out that all the other rotation operations can be obtained by combining the four fundamental rotations operations. As the first example, the improper rotation $s_n$ by $2\pi/n$ is the combination of $C_{nz}$ and $\sigma_h$. The second example is the rotation operation along $x$-axis, $C_{2x}$ for instance, which can be considered as the reflection $\sigma_x$ ($xz$ plane as the reflection plane) followed by $\sigma_h$.

According to the relationship of generating functions and electromagnetic multipoles, we summarize the symmetry properties of electromagnetic multipoles in Table 1 which comprehensively

Optics EXPRESS

tabulates the constraints on the electric and magnetic multipoles imposed by the two fundamental symmetric operations in 2D, and four fundamental symmetric operations in 3D. As a side remark, the rotation operation $C_{nz}$ only affects the order $m$ in electromagnetic multipoles, while the symmetric operation $\sigma_v$ impose the constraints on the electromagnetic multipoles with opposite $m$. From Table 1, one also notes that the parity of between electric and magnetic multipoles is different in the presence of $\sigma_h$ or $I$. For improper rotations, the constraints of electric multipoles and magnetic multipoles are opposite, which will be illustrated via explicit constraints through two exemplary scatterers with $C_{4v}$ or $D_{3h}$.

**Table 1. Symmetry properties of multipoles**

| Operation | | Electric multipoles | | Magnetic multipoles | |
|---|---|---|---|---|---|
| | | Symmetry | Antisymmetry | Symmetry | Antisymmetry |
| 2D | $C_{nz}$ | $m = Nn$ | $m = \left(N + \frac{1}{2}\right) n$ | $m = Nn$ | $m = \left(N + \frac{1}{2}\right) n$ |
| | $\sigma_v$ | $a_{-m} = a_m$ | $a_{-m} = -a_m$ | $b_{-m} = -b_m$ | $b_{-m} = b_m$ |
| 3D | $C_{nz}$ | $m = Nn$ | $m = \left(N + \frac{1}{2}\right) n$ | $m = Nn$ | $m = \left(N + \frac{1}{2}\right) n$ |
| | $\sigma_v$ | $\frac{a_{(l,-m)}}{a_{(l,m)}} = (-1)^m$ | $\frac{a_{(l,-m)}}{a_{(l,m)}} = (-1)^{m+1}$ | $\frac{b_{(l,-m)}}{b_{(l,m)}} = (-1)^{m+1}$ | $\frac{b_{(l,-m)}}{b_{(l,m)}} = (-1)^m$ |
| | $\sigma_h$ | $(l + m)$ even | $(l + m)$ odd | $(l + m)$ odd | $(l + m)$ even |
| | $I$ | $l$ even | $l$ odd | $l$ odd | $l$ even |

Both in 2D and 3D, the relation between $+m$ and $-m$ order imposed by $\sigma_v$ is only valid for $m \neq 0$.

### 2.4. The symmetry-adapted electromagnetic multipoles for symmetric scatterers

We further employ the standard group approach to classify the symmetry-adapted electromagnetic multipoles, for a given scattering object with regular geometry that can be described by a certain point group in either 2D or 3D. To that end, we search a certain combination of electromagnetic multipoles for each eigenfield of the scattering object, which can be assigned to one of the irreducible representations of the point group $G$. The explicit classification procedure has three steps. In the first step, we consider an eigenfield expanded by a series of modified generating functions, i.e, $\psi = \sum_{l,m} a_{(l,m)}\tilde{\psi}$ ($\psi = \sum_m a_m\tilde{\psi}_m$), which can be transformed into electromagnetic multipoles via the operators $\hat{O}_M$ and $\hat{O}_N$. In the second step, we use the projection operator [35] acting on the eigenfield $\psi$, where the projection operator is given as follows,

$$P^i = \frac{l_i}{g} \sum_{R \in G} \chi^i(R)^* P_R, \tag{13}$$

where $l_i$ is the dimension of the $i$-th irreducible representation of the group $G$ with order $g$, $\chi^i(R)^*$ is the character associated with the symmetric operator $P_R$ of group element $R$ and $R \in G$. In the last step, any rotational symmetry operations associated with the point group $G$ can be decomposed into the fundamental symmetry operations as listed in Table 1. As such, one can use the projection operator to find out the symmetry-adapted electromagnetic multipoles, from which the constraints on the expansion coefficients of electromagnetic multipoles can be extracted, see an example in Appendix C. In the following, the classification procedure is applied separately to a 2D scatterer with $C_{4v}$ symmetry and a 3D scatterer with $D_{3h}$ symmetry.

## 3. Results and discussion

### 3.1. Symmetric scatterers with $C_{4v}$ symmetry

Here we consider the eigenmodes associated with a 2D scattering object with a $C_{4v}$ rotational symmetry. The character table of the $C_{4v}$ group is shown in Table 2. In $C_{4v}$, there are four 1D

Optics EXPRESS

irreducible representations and one 2D irreducible representation, see row 2 - row 6 in Table 2. Each row from row 2 to row 6 corresponds to an irreducible representation, which can be assigned to the corresponding eigenmode expanded in terms of electromagnetic multipoles of the scatterer. With the assistance of the projection operator, i.e., $P^i$, one is able to build up the connections among the different multipoles for each irreducible representation, as tabulated in Table 2.

**Table 2. Character table of $C_{4v}$ and constraints on electromagnetic multipoles**

| $C_{4v}$ | $E$ | $C_2$ | $2C_4$ | $2\sigma_v$ | $2\sigma_d$ | Electric multipoles | Magnetic multipoles |
|---|---|---|---|---|---|---|---|
| $A_1$ | 1 | 1 | 1 | 1 | 1 | $m = 4N$, $a_{-m} = a_m$ | $m = 4N$, $b_{-m} = -b_m$ |
| $A_2$ | 1 | 1 | 1 | −1 | −1 | $m = 4N$, $a_{-m} = -a_m$ | $m = 4N$, $b_{-m} = b_m$ |
| $B_1$ | 1 | 1 | −1 | 1 | −1 | $m = 2 + 4N$, $a_{-m} = a_m$ | $m = 2 + 4N$, $b_{-m} = -b_m$ |
| $B_2$ | 1 | 1 | −1 | −1 | 1 | $m = 2 + 4N$, $a_{-m} = -a_m$ | $m = 2 + 4N$, $b_{-m} = b_m$ |
| $E$ | 2 | −2 | 0 | 0 | 0 | $m = 1 + 2N$, $\gamma = \pi$ | $m = 1 + 2N$, $\gamma = \pi$ |

$\gamma = \left[\arg\left(a^1_{4N_1+1}\right) - \arg\left(a^1_{4N_2-1}\right)\right] - \left[\arg\left(a^2_{4N_1+1}\right) - \arg\left(a^2_{4N_2-1}\right)\right]$ and $a$ is replaced with $b$ for magnetic multipoles.

All the operations can be obtained from the group generators or the combined operations of the group generators, thus it is sufficient to just examine the constrains of multipoles from the symmetry operations of the group generators. For example, there are 8 elements in the group $C_{4v}$, while the number of the generators of $C_{4v}$ is just 2, i.e., $C_4$ and $\sigma_v$. Indeed, the four 1D representations can be distinguished only by considering the generators $C_4$ and $\sigma_v$, forming the character table of $C_{4v}$. Thus, the constraints from symmetry considerations for the four 1D representations boil down to the requirements imposed only by $C_4$ and $\sigma_v$, leading to the selected value of $m$ ($m = 4N$) and the phase relations between $a_m$ and $a_{-m}$. Evidently, we make full wave simulation with a cross structure with group $C_{4v}$ in COMSOL Multiphysics as shown in Fig. 1, where the modal profiles of $E_z$ or $H_z$ are shown in Figs. 1(a)–1(d) and the $a$ or $b$ coefficients are plotted in Figs. 1(e)–1(h). Figures 1(a) and 1(b) illustrate the pure electric and magnetic multipoles of $B_2$ representation respectively, and the corresponding $a$ or $b$ coefficients of electromagnetic multipoles are presented in the second row of Fig. 1.

As for the 2D irreducible representations, there are two degenerate modes, which are orthogonal and form the basis. Without loss of generality, we take the two degenerate modes shown in Figs. 1(c) and 1(d) as the modal basis for the 2D irreducible representation. Under such circumstance, the matrix representations of each group elements can be given explicitly. For instance, choosing the red lines as the mirror plane for $\sigma_{v_1}$ and $\sigma_{v_2}$ in class $2\sigma_v$, the matrix representations of two generators are given by $C_4 = \begin{pmatrix} 0 & -1 \\ 1 & 0 \end{pmatrix}$ and $\sigma_{v_1} = \begin{pmatrix} -1 & 0 \\ 0 & 1 \end{pmatrix}$. By acting $C_4$ twice, one can get $C_2 = \begin{pmatrix} -1 & 0 \\ 0 & -1 \end{pmatrix}$, which indicates that the two degenerate eigenmodes shown in Figs. 1(c) and 1(d) are anti-symmetric under $C_2$ operation. Moreover, the symmetric properties of $C_2$ requires that $m$ must be an odd number. One also notes that the two generators $\sigma_v$ and $C_4$ share the same character for the $E$ representation. The symmetry operation in $2\sigma_v$ requires a phase relation between $\pm m$ electromagnetic multipoles within one mode, while the symmetry operation in $2C_4$ give rise to the connections between the two degenerate modes. The aforementioned two requirements can be combined and generalized into a single relation as $\gamma = \left[\arg\left(a^1_{4N_1+1}\right) - \arg\left(a^1_{4N_2-1}\right)\right] - \left[\arg\left(a^2_{4N_1+1}\right) - \arg\left(a^2_{4N_2-1}\right)\right] = \pi$ ($a$ is replaced with $b$ in magnetic multipoles), where the superscript represents two degenerate modes, $N_1$ and $N_2$ are integers. Though our discussions are based on the eigenmodes shown in Figs. 1(c) and

Optics EXPRESS

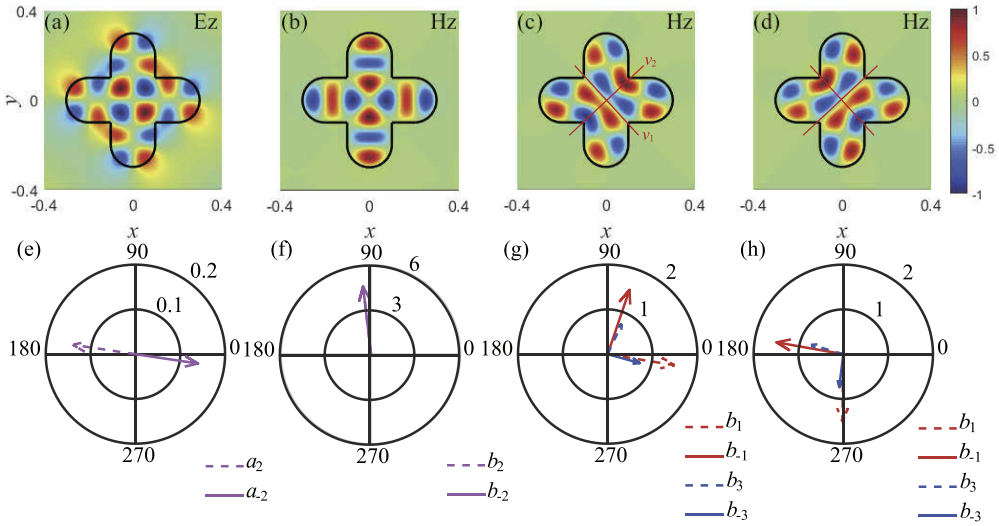


**Fig. 1.** The profile (a-d) and multipoles composition (e-h) of four different modes in the 2D cruciform scatterer with $C_{4v}$ symmetry. Only the first mode (a) is TM mode, and other three modes are TE modes. The first two modes (a,b) are both representation $B_2$ where $a_2 = -a_{-2}$ in (e) and $b_{-2} = b_2$ in (f). (c,d) are a pair of degenerate modes with $E$ representation, and the red lines represent the mirror plane of operation in $2\sigma_v$. The phase between four magnetic multipoles $b_{\pm1}$ and $b_{\pm3}$ in (g) or (f) are different, however, it is easy to check $\gamma = \pi$ ($\left[\arg\left(b_1^1\right) - \arg\left(b_{-1}^1\right)\right] - \left[\arg\left(b_1^2\right) - \arg\left(b_{-1}^2\right)\right] = \pi$ and $\left[\arg\left(b_1^1\right) - \arg\left(b_3^1\right)\right] - \left[\arg\left(b_1^2\right) - \arg\left(b_3^2\right)\right] = \pi$).

1(d), the single relation $\gamma = \pi$ summarized here is general and independent of the modal basis, due to the fact that rotating the eigenmode basis only modifies the explicit forms of matrix representations of the symmetry operators without modification of the characters, i.e., the trace of matrix representations for each symmetric operation is unchanged.

### 3.2. Symmetric scatterers with $D_{3h}$ symmetry

We continue to discuss and interpret the constraints of electromagnetic multipoles obtained from the aforementioned group approach for a triangular prism with equilateral triangle section, which is a 3D scatter with the $D_{3h}$ symmetry. The character table and the constraints of electromagnetic multipoles are listed in Table 3. In contrast to $C_{4v}$, there are 6 irreducible representations in $D_{3h}$ group, i.e., 4 1D representations and 2 2D representations, as listed in the row 2 - row 7 shown in Table 3. The group $D_{3h}$ can be seen as the direct product of group $C_{1h}$ and $D_3$, i.e., $D_{3h} = D_3 \otimes C_{1h}$. Therefore, both the group generator of $C_{1h}$ and those of $D_3$ are the generators of $D_{3h}$, i.e., $\sigma_h$, $C_3$ and $C_2'$. Notably, $\sigma_h$ is the generator of $C_{1h}$, which is the generator of $D_{3h}$ that distinguishes the 1D and 2D irreducible representations as shown in Table 3. The other two group generators, i.e., $C_3$ and $C_2'$ ($\pi$ rotation with axial in horizontal plane), together distinguish the 4 1D representations of $D_{3h}$ as displayed in Table 3. Since $C_2'$ can be seen as two successive operations, i.e., $\sigma_v$ followed by $\sigma_h$, we can replace $C_2'$ with $\sigma_v$ as generator in $D_{3h}$ for convenience. As a result, we can use the similar approach to interpret the four 1D representations in $D_{3h}$ as those in $C_{4v}$. In Figs. 2(a)–2(d), we show two eigenmodes of different representation. Figures 2(a) and 2(c) represent the first mode and rest figures represent the other. We choose different planes to show the features of the modes in complex 3D scatterers. The group theory method is still valid in the 3D situation. In Figs. 2(a) and 2(b), we choose $xy$ plane which displays the impact

Optics EXPRESS

of $\sigma_v$ and $C_3$ on $E_z$. The field distribution of $E_z$ in the one mode is unchanged and the other is inverse under the operation $\sigma_v$. In Figs. 2(c) and 2(d), we choose $yz$ plane which displays the impact of $\sigma_h$ on $E_y$, we get two modes of different representations because the character of $\sigma_v$ operation for the first modes is -1 and the second is 1.

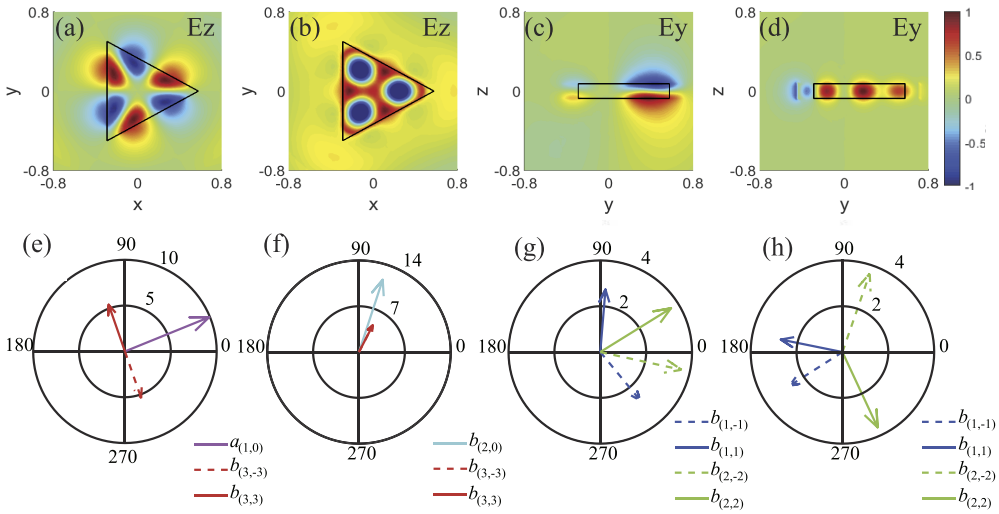


**Fig. 2.** The modal profiles (a-d) and multipolar decomposition (e-h) for the eigenmodes of the scatterer with $D_{3h}$ symmetry. (a,b) The field distribution of $E_z$ in x-y plane, the character of $\sigma_v$ operation for mode shown in (a)/(b) is -1/1; (c,d) the field distribution of $E_y$ in y-z plane, the character of $\sigma_h$ operation for mode shown in (c)/(d) is -1/1. (e,f) The multipolar coefficients of the modes with 1D representation, where the first mode has non-zero $a_{(1,0)}$ and $b_{(3,-3)} = -b_{(3,3)}$, and the second mode has non-zero $b_{(2,0)}$ and $b_{(3,-3)} = b_{(3,3)}$. (g,h) The multipolar coefficients of a pair of degenerate modes, with special requirements on the order m and the phase correlations between different multipoles.

By definition, as the projection operation $P$ of a certain representation is projected onto the eigenmode with the exactly same representation, we get the eigenmode itself with proper normalization, otherwise we get null projection for the eigenmodes with different representations. Thereby, we firstly act each projection operation, i.e., see the entities in the first row of Table 3, onto the corresponding eigenmode to obtain the constraints of electric and magnetic multipoles, as listed in the 8th and 9th column in Table 3 respectively. Next, we perform the numerical calculations of the eigenmodes using finite element method (FEM) of the same scatter as examined in Table 3 and further implement the multipolar decomposition numerically, the multipolar coefficients of which are shown in Figs. 2(e)–2(h). Lastly, we analyze the multipolar components of the eigenmodes of the scatterer with $D_{3h}$ symmetry from two independent approaches, our group approach and the FEM modelling. As an example, the numerical electromagnetic multipole decomposition of the eigenmode with $A_1''$ representation shown in Fig. 2(e) leads to the following results: (1) the existence of non-zero $a_{(1,0)}$, (2) $b_{(3,-3)} = -b_{(3,3)}$. As for the electric multipole $M_{(1,0)}$, i.e., $m = 0$ and $l + m$ odd, it is straightforward to verify that the electromagnetic multipoles indeed fulfill the requirements given in the Table 3 for $A_1''$ representation. Moreover, as for the magnetic multipole $N_{l=3,m=\pm3}$, i.e., $m = 3$, $b_{(3,-3)} = -b_{(3,3)}$ and $l + m$ even, the relative relations between the $N_{l=3,m=3}$ and $N_{l=3,m=-3}$ is also consistent with the constraints of the magnetic multipoles given in Table 3 for $A_1''$ representation. The same conclusion can be drawn for the eigenmode with $A_2''$ representation, see the numerical electromagnetic multipole decomposition in Fig. 2(f) and the corresponding constraints in Table 3.

Optics EXPRESS

**Table 3. Character table of $D_{3h}$ and constraint of multipoles**

| $D_{3h}$ | $E$ | $\sigma_h$ | $2C_3$ | $2s_3$ | $3C_2'$ | $3\sigma_v$ | Electric multipoles | Magnetic multipoles |
|---|---|---|---|---|---|---|---|---|
| $A_1'$ | 1 | 1 | 1 | 1 | 1 | 1 | $m = 3N$, $(l+m)$ even, $a_{(l,-m)} = (-1)^m a_{(l,m)}$ | $m = 3N$, $(l+m)$ odd, $b_{(l,-m)} = (-1)^{m+1} b_{(l,m)}$ |
| $A_2'$ | 1 | 1 | 1 | 1 | −1 | −1 | $m = 3N$, $(l+m)$ even, $a_{(l,-m)} = (-1)^{m+1} a_{(l,m)}$ | $m = 3N$, $(l+m)$ odd, $b_{(l,-m)} = (-1)^m b_{(l,m)}$ |
| $A_1''$ | 1 | −1 | 1 | −1 | 1 | −1 | $m = 3N$, $(l+m)$ odd, $a_{(l,-m)} = (-1)^{m+1} a_{(l,m)}$ | $m = 3N$, $(l+m)$ even, $b_{(l,-m)} = (-1)^m b_{(l,m)}$ |
| $A_2''$ | 1 | −1 | 1 | −1 | −1 | 1 | $m = 3N$, $(l+m)$ odd, $a_{(l,-m)} = (-1)^m a_{(l,m)}$ | $m = 3N$, $(l+m)$ even, $b_{(l,-m)} = (-1)^{m+1} b_{(l,m)}$ |
| $E'$ | 2 | 2 | −1 | −1 | 0 | 0 | $m = 3N \pm 1$, $\gamma = \pi$, $(l+m)$ even | $m = 3N \pm 1$, $\gamma = \pi$, $(l+m)$ odd |
| $E''$ | 2 | −2 | −1 | 1 | 0 | 0 | $m = 3N \pm 1$, $\gamma = \pi$, $(l+m)$ odd | $m = 3N \pm 1$, $\gamma = \pi$, $(l+m)$ even |

$\gamma = \left[\arg\left(a^1_{3N_1+1}\right) - \arg\left(a^1_{3N_2-1}\right)\right] - \left[\arg\left(a^2_{3N_1+1}\right) - \arg\left(a^2_{3N_2-1}\right)\right] = \pi$ and $a$ is replaced with $b$ for magnetic multipoles.

As for two degenerate modes in Figs. 2(g) and 2(h), we use a similar approach in the 2D scenario by using the explicit modal basis, which essentially contains and only contains the two degenerate modes. Subsequently, we apply the projection operator $P(E'')$ onto the eigenmodes with the representation $E''$ to obtain the corresponding constraints of the electromagnetic multipoles. Again, the numerical decomposition of electromagnetic multipoles from FEM calculation, i.e., $(l+m)$ is odd and even for electric and magnetic multipoles respectively, $m = 3N \pm 1$ and the phase locking between these electromagnetic multipoles, is consistent with the constraints given in the Table 3. For the eigenmodes with the other representations, one can further easily check that the constraints of the electromagnetic multipoles imposed by group symmetry are in perfect agreements with the numerical simulations of the eigenmodes obtained from FEM modelling.

## 4. Conclusion

In conclusion, we provide a comprehensive and systematic classification on the symmetric relations among the electromagnetic multipoles for the geometrically regular scatterers. The key in classifying the vector field of the optical eigenmodes expanded in terms of electromagnetic multipoles for symmetric scatterers is to introduce the generating functions, by which the standard group approach can be applied. Explicitly, we associate the eigenmodes of symmetric scatterers to individual irreducible representation of the corresponding symmetry group, which contains a number of fundamental symmetry operations that give rise to the constraints of the electromagnetic multipoles due to symmetry arguments. We tabulate all the fundamental symmetry operations both in 2D and 3D, as well as the constrains on the electromagnetic multipoles. We further apply our group approach to examine the symmetric relation for the electromagnetic multipoles of a 2D scatterer with $C_{4v}$ symmetry and that of a 3D scatterer with $D_{3h}$ symmetry, both of which are in perfect agreements with FEM fullwave simulations.

The language of electromagnetic multipoles is a fundamental tool to analyze the scattering and farfield pattern, thereby is important and useful for engineering scattering far field or beam steering. Using our method, without implementing any numerical calculations of geometrically complex

Optics EXPRESS

but symmetric scatterers, one is able to know the symmetry relations among electromagnetic multipoles, which is very convenient and instructive. Considering the fundamental role of group approach in physics as well as that of electromagnetic multipoles in scattering problems, we believe that the theoretical construction based on the group theory is rather generic, and provide insightful information about light scattering by symmetric scatterers, and thus can be useful in designing the geometry of scattering object for directional emission or meta-atoms with more advanced functionalities in meta-surfaces.

## Appendix A: The symmetry relationship between modified generating functions $\tilde{\psi}_{(l,m)}$ and electromagnetic multipoles $\boldsymbol{N}_{(l,m)}$, $\boldsymbol{M}_{(l,m)}$

We demonstrate 3D case for instance. When any proper rotation operator $\hat{O}_R$ acts on magnetic multipole $\boldsymbol{M}_{(l,m)} = \boldsymbol{r} \times \nabla\tilde{\psi}_{(l,m)}$, we have $\hat{O}_R\boldsymbol{M}_{(l,m)} = \tilde{R}\left[\boldsymbol{r}' \times \nabla_{\boldsymbol{r}'}\tilde{\psi}_{(l,m)}(\boldsymbol{r}')\right]$ where $\boldsymbol{r}' = \tilde{R}^{-1}\boldsymbol{r}$ and

$$\tilde{R} = \begin{pmatrix} \cos\alpha\cos\beta\cos\gamma - \sin\alpha\sin\gamma & -\cos\alpha\cos\beta\sin\gamma - \sin\alpha\cos\gamma & \cos\alpha\sin\beta \\ \sin\alpha\cos\beta\cos\gamma + \cos\alpha\sin\gamma & -\sin\alpha\cos\beta\sin\gamma + \cos\alpha\cos\gamma & \sin\alpha\sin\beta \\ -\sin\beta\cos\gamma & \sin\beta\sin\gamma & \cos\beta \end{pmatrix} \tag{14}$$

is re group $SO(3)$, where $\alpha$ $\beta$ and $\gamma$ are Euler angles. Since $\hat{O}_M\hat{O}_R\tilde{\psi}_{(l,m)} = \boldsymbol{r} \times \nabla_{\boldsymbol{r}}\tilde{\psi}_{(l,m)}(\boldsymbol{r}') = \left(\tilde{R}\boldsymbol{r}'\right) \times \left[\tilde{R}\nabla_{\boldsymbol{r}'}\tilde{\psi}_{(l,m)}(\boldsymbol{r}')\right]$ with $\nabla_{\boldsymbol{r}} = \tilde{R}\nabla_{\boldsymbol{r}'}$, it is easy to prove that $\hat{O}_R\boldsymbol{M}_{(l,m)} - \hat{O}_M\hat{O}_R\tilde{\psi}_{(l,m)} = 0$. Any improper rotation can be seen as inversion $\hat{I}$ adds to proper rotation $\hat{O}_R$ and $\hat{I}\tilde{R} = -\tilde{R}$, thus $\hat{I}\hat{O}_R\boldsymbol{M}_{(l,m)} + \hat{O}_M\hat{I}\hat{O}_R\tilde{\psi}_{(l,m)} = 0$. In similar way, we can get the commutation between $\hat{O}_R$ and $\nabla\times$, $\hat{O}_R(\nabla \times \boldsymbol{f}) - \nabla \times \left(\hat{O}_R\boldsymbol{f}\right) = \tilde{R}\left[\nabla_{\boldsymbol{r}'} \times \boldsymbol{f}(\boldsymbol{r}')\right] - \left(\tilde{R}\nabla_{\boldsymbol{r}'}\right) \times \left[\tilde{R}\boldsymbol{f}(\boldsymbol{r}')\right] = 0$ where $\boldsymbol{f}$ is any vector. By replacing $\tilde{R}$ to $-\tilde{R}$, it is easy to prove that $\nabla\times$ anticommutes with $\hat{I}\hat{O}_R$.

## Appendix B: The relationship of $\pm m$ order of the modified generating functions

The reflection $\sigma_v$ in a vertical plane can transform $m$ order electromagnetic multipole to $-m$ order electromagnetic multipole is based on the relationship between $\pm m$ of modified generating functions. Since there is no $-m$ order electromagnetic multipoles when $m = 0$, this case is excluded in this section. With the relationship of Bessel (Hankel) function $Z_{-m} = (-1)^m Z_m$, we have

$$\tilde{\psi}_{-m} = (-i)^{-m} Z_{-m}(kr)\, e^{-im\phi} = (-i)^m Z_m(kr)\, e^{-im\phi} = e^{-2m\phi}\tilde{\psi}_m. \tag{15}$$

By using the relationship of associated Legendre function $P_l^{-m} = (-1)^m \frac{(l-m)!}{(l+m)!} P_l^m$, we get

$$\begin{aligned} \tilde{\psi}_{(l,-m)} &= i^l \frac{\sqrt{(2l+1)(l+m)!}}{\sqrt{l(l+1)(l-m)!}} e^{-im\phi} P_l^{-m}(\cos\theta)\, z_l(kr) \\ &= i^l (-1)^m \frac{\sqrt{(2l+1)(l-m)!}}{\sqrt{l(l+1)(l+m)!}} e^{-im\phi} P_l^m(\cos\theta)\, z_l(kr) = (-1)^m e^{-2m\phi}\tilde{\psi}_{(l,m)}. \end{aligned} \tag{16}$$

## Appendix C: An example of using projection operator to get the symmetry-adapted multipoles

For instance, the projection operator of representation $A_2'$ in Group $D_{3h}$ is

$$\begin{aligned} P\left(A_2'\right) = \frac{1}{12}\Big(&P_E + P_{\sigma_h} + P_{C_{3z}} + P_{C_{3z}^{-1}} + P_{s_3} + P_{s_3^{-1}} \\ &- P_{c'_2} - P_{c''_2} - P_{c'''_2} - P_{\sigma_{v1}} - P_{\sigma_{v2}} - P_{\sigma_{v3}}\Big), \end{aligned} \tag{17}$$

Optics EXPRESS

when it acts on $\psi = \sum_{l,m} a_{(l,m)}\tilde{\psi}_{(l,m)}$ we get the basis function of $A_2'$

$$
\begin{aligned}
\psi\left(A_2'\right) = P\left(A_2'\right)\psi &= \frac{3}{12}\left[(-1)^l + 1\right] a_{(l,0)}\tilde{\psi}_{(l,0)} \\
&+ \frac{1}{12}\sum_{l,m\neq 0}\left[(-1)^{l+m} + 1\right]\left[1 + e^{-im\frac{2\pi}{3}} + e^{im\frac{2\pi}{3}}\right] a_{(l,m)}\tilde{\psi}_{(l,m)} \\
&- \frac{1}{12}\sum_{l,m\neq 0}\left[(-1)^m + (-1)^l\right]\left[1 + e^{im\frac{4\pi}{3}} + e^{-im\frac{4\pi}{3}}\right] e^{i2m\phi_0} a_{(l,m)}\tilde{\psi}_{(l,-m)} \\
=&\frac{1}{4}\left[(-1)^l + 1\right] a_{(l,0)}\tilde{\psi}_{(l,0)} + \frac{1}{12}\sum_{l,m\neq 0}\left[(-1)^{l+m} + 1\right]\left[1 + 2\cos\left(m\frac{2\pi}{3}\right)\right] a_{(l,m)}\tilde{\psi}_{(l,m)} \\
&- \frac{1}{12}\sum_{l,m\neq 0}\left[(-1)^{l+m} + 1\right]\left[1 + 2\cos\left(m\frac{4\pi}{3}\right)\right] e^{m(\pi - i2\phi_0)} a_{(l,-m)}\tilde{\psi}_{(l,m)} \\
=&\frac{1}{4}\left[(-1)^l + 1\right] a_{(l,0)}\tilde{\psi}_{(l,0)} \\
&+ \frac{1}{12}\sum_{l,m}\left[(-1)^{l+m} + 1\right]\left[1 + 2\cos\left(m\frac{2\pi}{3}\right)\right]\left[a_{(l,m)} - e^{im(\pi - 2\phi_0)} a_{(l,-m)}\right]\tilde{\psi}_{(l,m)}.
\end{aligned}
\tag{18}
$$

Therefore, when $l + m =$ even or $m = 3N$ the coefficient of electromagnetic multipole is zero. By changing $m$ to $-m$, we find the coefficients between $\pm m$ order multipoles have same absolute value and a phase difference $-e^{im(2\phi_0 - \pi)}$. In addition, the projection can only find one of basis functions of high order representation, the rest of them should be acquired by orthogonality and normalization.

## Funding

National Natural Science Foundation of China ((11874026, 61735006, 61775063); National Basic Research Program of China (973 Program) (2017YFA0305200); Fundamental Research Funds for the Central Universities (HUST: 2017KFYXJJ027, HUST: 2018KFYYXJJ055).

## Disclosures

The authors declare no conflicts of interest.

## References


1. M. Lax, *Symmetry principles in solid state and molecular physics* (Courier Corporation, 2001).
2. W.-K. Tung, *Group theory in physics: an introduction to symmetry principles, group representations, and special functions in classical and quantum physics* (World Scientific Publishing Company, 1985).
3. A. Gelessus, W. Thiel, and W. Weber, "Multipoles and symmetry," J. Chem. Educ. **72**(6), 505 (1995).
4. E. Wigner, *Group theory: and its application to the quantum mechanics of atomic spectra*, vol. 5 (Elsevier, 2012).
5. R. El-Ganainy, K. G. Makris, M. Khajavikhan, Z. H. Musslimani, S. Rotter, and D. N. Christodoulides, "Non-hermitian physics and pt symmetry," Nat. Phys. **14**(1), 11–19 (2018).
6. X. Zhu, H. Ramezani, C. Shi, J. Zhu, and X. Zhang, "$\mathcal{PT}$-symmetric acoustics," Phys. Rev. X **4**(3), 031042 (2014).
7. Z. Xiong, W. Chen, P. Wang, and Y. Chen, "Classification of symmetry properties of waveguide modes in presence of gain/losses, anisotropy/bianisotropy, or continuous/discrete rotational symmetry," Opt. Express **25**(24), 29822–29834 (2017).
8. L. Fu and C. L. Kane, "Topological insulators with inversion symmetry," Phys. Rev. B **76**(4), 045302 (2007).
9. M. C. Rechtsman, J. M. Zeuner, Y. Plotnik, Y. Lumer, D. Podolsky, F. Dreisow, S. Nolte, M. Segev, and A. Szameit, "Photonic floquet topological insulators," Nature **496**(7444), 196–200 (2013).
10. K. Sakoda, "Symmetry, degeneracy, and uncoupled modes in two-dimensional photonic lattices," Phys. Rev. B **52**(11), 7982–7986 (1995).
11. K. Sakoda and H. Zhou, "Analytical study of two-dimensional degenerate metamaterial antennas," Opt. Express **19**(15), 13899–13921 (2011).

Optics EXPRESS


12. K. Sakoda, *Optical properties of photonic crystals*, vol. 80 (Springer Science & Business Media, 2004).
13. J. D. Joannopoulos, S. G. Johnson, J. N. Winn, and R. D. Meade, *Photonic Crystals-Molding the flow of light* (Princeton Univeristy Press, 1995).
14. R. Wang, X.-H. Wang, B.-Y. Gu, and G.-Z. Yang, "Effects of shapes and orientations of scatterers and lattice symmetries on the photonic band gap in two-dimensional photonic crystals," J. Appl. Phys. **90**(9), 4307–4313 (2001).
15. J.-F. Liu, H.-X. Jiang, C.-J. Jin, X.-H. Wang, Z.-S. Gan, B.-H. Jia, and M. Gu, "Orientation-dependent local density of states in three-dimensional photonic crystals," Phys. Rev. A **85**(1), 015802 (2012).
16. J. F. Wheeldon, T. Hall, and H. Schriemer, "Symmetry constraints and the existence of bloch mode vortices in linear photonic crystals," Opt. Express **15**(6), 3531–3542 (2007).
17. Y. Zhang, A. Chen, W. Liu, C. W. Hsu, B. Wang, F. Guan, X. Liu, L. Shi, L. Lu, and J. Zi, "Observation of polarization vortices in momentum space," Phys. Rev. Lett. **120**(18), 186103 (2018).
18. W. Liu, B. Wang, Y. Zhang, J. Wang, M. Zhao, F. Guan, X. Liu, L. Shi, and J. Zi, "Circularly polarized states spawning from bound states in the continuum," Phys. Rev. Lett. **123**(11), 116104 (2019).
19. B. Zhen, C. W. Hsu, L. Lu, A. D. Stone, and M. Soljačić, "Topological nature of optical bound states in the continuum," Phys. Rev. Lett. **113**(25), 257401 (2014).
20. C. F. Bohren and D. R. Huffman, *Absorption and scattering of light by small particles* (John Wiley & Sons, 2008).
21. W. Chen, Y. Chen, and W. Liu, "Singularities and poincaré indices of electromagnetic multipoles," Phys. Rev. Lett. **122**(15), 153907 (2019).
22. A. E. Krasnok, C. R. Simovski, P. A. Belov, and Y. S. Kivshar, "Superdirective dielectric nanoantennas," Nanoscale **6**(13), 7354–7361 (2014).
23. A. I. Kuznetsov, A. E. Miroshnichenko, M. L. Brongersma, Y. S. Kivshar, and B. Luk'yanchuk, "Optically resonant dielectric nanostructures," Science **354**(6314), aag2472 (2016).
24. W. Liu, J. Zhang, B. Lei, H. Ma, W. Xie, and H. Hu, "Ultra-directional forward scattering by individual core-shell nanoparticles," Opt. Express **22**(13), 16178–16187 (2014).
25. D. Smirnova and Y. S. Kivshar, "Multipolar nonlinear nanophotonics," Optica **3**(11), 1241–1255 (2016).
26. A. E. Miroshnichenko and M. I. Tribelsky, "Ultimate absorption in light scattering by a finite obstacle," Phys. Rev. Lett. **120**(3), 033902 (2018).
27. S. Jahani and Z. Jacob, "All-dielectric metamaterials," Nat. Nanotechnol. **11**(1), 23–36 (2016).
28. W. Liu, "Ultra-directional super-scattering of homogenous spherical particles with radial anisotropy," Opt. Express **23**(11), 14734–14743 (2015).
29. W. Liu, A. E. Miroshnichenko, D. N. Neshev, and Y. S. Kivshar, "Broadband unidirectional scattering by magneto-electric core–shell nanoparticles," ACS Nano **6**(6), 5489–5497 (2012).
30. B. Hopkins, A. N. Poddubny, A. E. Miroshnichenko, and Y. S. Kivshar, "Revisiting the physics of fano resonances for nanoparticle oligomers," Phys. Rev. A **88**(5), 053819 (2013).
31. A. R. Edmonds, *Angular momentum in quantum mechanics*, vol. 4 (Princeton University Press, 1996).
32. G. Burns, *Introduction to group theory with applications: materials science and technology* (Academic Press, 2014), chap. 7, p. 138.
33. W. Hergert and M. Däne, "Group theoretical investigations of photonic band structures," Phys. Status Solidi A **197**(3), 620–634 (2003).
34. P. Grahn, A. Shevchenko, and M. Kaivola, "Electromagnetic multipole theory for optical nanomaterials," New J. Phys. **14**(9), 093033 (2012).
35. M. Tinkham, *Group theory and quantum mechanics* (Courier Corporation, 2003).